

**GENERALIZED LIMITS TO THE NUMBER OF LIGHT PARTICLE
DEGREES OF FREEDOM FROM BIG BANG NUCLEOSYNTHESIS**Keith A. Olive^a*University of Minnesota, School of Physics and Astronomy
Theoretical Physics Institute
116 Church St SE, Minneapolis, MN 55455*David Thomas^b*University of Chicago, Astronomy & Astrophysics Center
5640 S Ellis Ave, Chicago, IL 60637***Abstract**

We compute the big bang nucleosynthesis limit on the number of light neutrino degrees of freedom in a model-independent likelihood analysis based on the abundances of ^4He and ^7Li . We use the two-dimensional likelihood functions to simultaneously constrain the baryon-to-photon ratio and the number of light neutrinos for a range of ^4He abundances $Y_p = 0.225 - 0.250$, as well as a range in primordial ^7Li abundances from $(1.6 \text{ to } 4.1) \times 10^{-10}$. For $(^7\text{Li}/\text{H})_p = 1.6 \times 10^{-10}$, as can be inferred from the ^7Li data from Population II halo stars, the upper limit to N_ν based on the current best estimate of the primordial ^4He abundance of $Y_p = 0.238$, is $N_\nu < 4.3$ and varies from $N_\nu < 3.3$ (at 95% C.L.) when $Y_p = 0.225$ to $N_\nu < 5.3$ when $Y_p = 0.250$. If ^7Li is depleted in these stars the upper limit to N_ν is relaxed. Taking $(^7\text{Li}/\text{H})_p = 4.1 \times 10^{-10}$, the limit varies from $N_\nu < 3.9$ when $Y_p = 0.225$ to $N_\nu \lesssim 6$ when $Y_p = 0.250$. We also consider the consequences on the upper limit to N_ν if recent observations of deuterium in high-redshift quasar absorption-line systems are confirmed.

^aolive@mnhep.hep.umn.edu^bdavet@oddjob.uchicago.edu

1 Introduction

One of the most important limits on particle properties is the limit on the number of light particle degrees of freedom at the time of big bang nucleosynthesis (BBN) [1]. This is commonly computed as a limit on the number of light neutrino flavors, N_ν . Recently, we [2] used a model-independent likelihood method (see also [3, 4]) to simultaneously constrain the value of the one true parameter in *standard* BBN, the baryon-to-photon ratio η , together with N_ν . For similar approaches, see [5]. In that work [2], we based our results on the best estimate of the observationally determined abundance of ^4He , $Y_p = 0.234 \pm 0.002 \pm 0.005$ from [6], and of ^7Li , $^7\text{Li}/\text{H} = (1.6 \pm 0.1) \times 10^{-10}$, from [7]. While these determinations can still be considered good ones today, there is often discussion of higher abundance for ^4He as perhaps indicated by the data of [8] and higher abundances of ^7Li due to the effects of stellar depletion (see e.g. [9]). Rather than be forced to continually update the limit on N_ν as the observational situation evolves, we generalize our previous work here and compute the upper limit on N_ν for a wide range of possible observed abundances of ^4He and ^7Li . Because the determinations of D/H in quasar absorption system has not dramatically improved, we can only comment on the implications of either the high or low D/H measurements.

One of the major obstacles in testing BBN using the observed abundances of the light element isotopes rests on our ability to infer from these observations a primordial abundance. Because ^4He , in extragalactic HII regions, and ^7Li , in the atmospheres of old halo dwarf stars, are both measured in very low metallicity systems (down to 1/50th solar for ^4He and 1/1000th solar for ^7Li), very little modeling in the way of galactic chemical evolution is required to extract a primordial abundance for these isotopes. Of course systematic uncertainties, such as underlying stellar absorption, in determining the ^4He abundance and the effects of stellar depletion of ^7Li lead to uncertainties in the primordial abundances of these isotopes, and it is for that reason we are re-examining the limits to N_ν . Nevertheless, the problems in extracting a primordial ^4He and ^7Li abundance pale in comparison with those for D and ^3He , both of which are subject to considerable uncertainties not only tied to the observations, but to galactic chemical evolution. In fact, ^3He also suffers from serious uncertainties concerning its fate in low mass stars [10]. ^3He is both produced and destroyed in stars making the connection to BBN very difficult.

Deuterium is totally destroyed in the star formation process. As such, the present or solar abundance of D/H is highly dependent on the details of a chemical evolution model, and in particular the galactic star formation rate. Unfortunately, it is very difficult at the present time to gain insight on the primordial abundance of D/H from chemical evolution given present and solar abundances since reasonably successful models of chemical evolution can be constructed for primordial D/H values which differ by nearly an order of magnitude¹ [11].

Of course much of the recent excitement surrounding deuterium concerns the observation of D/H in quasar absorption systems [14]-[17]. If a single value for the D/H abundance in

¹There may be some indication from studies of the luminosity density at high redshift which implies a steeply decreasing star formation rate [12], and that at least on a cosmic scale, significant amounts of deuterium has been destroyed [13].

these systems could be established², then one could avoid all of the complications concerning D/H and chemical evolution, and because of the steep monotonic dependence of D/H on η , a good measurement of D/H would alone be sufficient to determine the value of η (since D/H is nearly independent of N_ν). In this case, the data from ^4He and ^7Li would be most valuable as a consistency test on BBN and in the case of ^4He , to set limits on particle properties. In the analysis that follows, we will discuss the consequences of the validity of either the high or low D/H determinations.

Using a likelihood analysis based on ^4He and ^7Li [4], a probable range for the baryon-to-photon ratio, η was determined. The ^4He likelihood distribution has a single peak due to the monotonic dependence of ^4He on η . However, because the dependence on η is relatively flat, particularly at higher values of Y_p , this peak may be very broad, yielding little information on η alone. On the other hand, because ^7Li is not monotonic in η , the BBN prediction has a minimum at $\eta_{10} \simeq 3$ ($\eta_{10} = 10^{10}\eta$) and as a result, for an observationally determined value of ^7Li above the minimum, the ^7Li likelihood distribution will show two peaks. The total likelihood distribution based on ^4He and ^7Li is simply the product of the two individual distributions. In [4], the best fit value for η_{10} based on the quoted observational abundances was found to be 1.8 with a 95% CL range

$$1.4 < \eta_{10} < 4.3 \tag{1}$$

when restricting the analysis to the standard model, including $N_\nu = 3$. In determining (1) systematic errors were treated as Gaussian distributed. When D/H from quasar absorption systems (those showing a high value for D/H [14, 16]) is included in the analysis this range is cut to $1.50 < \eta_{10} < 2.55$.

In [2], the maximum likelihood analysis of [3, 4] which utilized a likelihood function $\mathcal{L}(\eta)$ for fixed $N_\nu = 3$ was generalized to allow for variability in N_ν . There a more general likelihood function $\mathcal{L}(\eta, N_\nu)$ was applied to the current best estimates of the primordial ^4He and ^7Li abundances. Based on the analysis in [6], we chose $Y_p = 0.234 \pm 0.002(\text{stat.}) \pm 0.005(\text{syst.})$ as well as the lower value $Y_p = 0.230 \pm 0.003(\text{stat.}) \pm 0.005(\text{syst.})$ based on a low metallicity subset of the data. Using these values of Y_p along with the value $(\text{Li}/\text{H})_p = (1.6 \pm 0.07) \times 10^{-10}$ from [7], we found peak likelihood values $\eta_{10} = 1.8$ and $N_\nu = 3.0$ with a 95% CL range of $1.6 \leq N_\nu \leq 4.0, 1.3 \leq \eta_{10} \leq 5.0$ for the higher ^4He value and similar results for the lower one. More recent data from Izotov and Thuan [19] seems to indicate a still higher value for Y_p , and for this reason as well as wishing to be independent of the “*current*” best estimate of the abundances, we derive our results for a wide range of possible values for Y_p and $(\text{Li}/\text{H})_p$ which will account for the possibility of stellar depletion for the latter [9]. Finally, in [2], we considered only the effect of the high D/H value from quasar absorption systems. Since there was virtually no overlap between the likelihood functions based on the low D/H value and the other two elements, there was little point in using that value in our analysis. Since then, the low D/H value has been raised somewhat, and that together with our present consideration of higher Y_p and $(\text{Li}/\text{H})_p$ values makes the exercise worth while.

²It is not possible that all disparate determinations of D/H represent an inhomogeneous primordial abundance as the corresponding inhomogeneity in η would lead to anisotropies in the microwave background in excess of those observed [18].

In this paper, we follow the approach of [2] – [4] in constraining the theory on the basis of the ^4He and ^7Li data and to a lesser extent D/H , by constructing a likelihood function $\mathcal{L}(\eta, N_\nu)$. We discuss the current status of the data in section 2, and indicate what range of values for the primordial abundances we consider. In section 3, we display the likelihood functions we use. As this was discussed in more detail in [2, 4], we will be brief here. Our results are given in section 4, and we draw conclusions in section 5.

2 Observational Data

Data pertinent to the primordial ^4He abundance is obtained from observations of extragalactic HII regions. These regions have low metallicities (as low as 1/50th solar), and thus are presumably more primitive than similar regions in our own Galaxy. The ^4He abundance used to extract a primordial value spans roughly an order of magnitude in metallicity (e.g. O/H). Furthermore, since there have been a considerable number of such systems observed with metallicities significantly below solar, modeling plays a relatively unimportant role in obtaining the primordial abundance of ^4He (see e.g. [20]).

The ^4He data based on observations in [21, 8] were discussed in detail in [6]. There are over 70 such regions observed with metallicities ranging from about 2–30% of solar metallicity. This data led to the determination of a primordial ^4He abundance of $Y_p = 0.234 \pm 0.002(\text{stat.}) \pm 0.005(\text{syst.})$ used in [2]. That the statistical error is small is due to the large number of regions observed and to the fact that the ^4He abundance in these regions is found to be very well correlated to metallicity. In fact, as can be understood from the remarks which follow, the primordial ^4He abundance is dominated by systematic rather than statistical uncertainties.

The compilation in [6] included the data of [8]. Although this data is found to be consistent with other data on a point by point basis, taken alone, it would imply a somewhat higher primordial ^4He abundance. Furthermore, the resulting value of Y_p depends on the method of data analysis. When only ^4He data is used to self-consistently determine the ^4He abundance (as opposed to using other data such as oxygen and sulphur to determine the parameters which characterize the HII region and are needed to convert an observation of a ^4He line strength into an abundance), a value of Y_p as high as 0.244 ± 0.002 can be found³ [8].

The problem concerning ^4He has been accentuated recently with new data from Izotov and Thuan [19]. The enlarged data set from [21, 19] was considered in [20]. The new resulting value for Y_p is

$$Y_p = 0.238 \pm 0.002(\text{stat.}) \pm 0.005(\text{syst.}) \quad (2)$$

The new data taken alone gives $Y_p = 0.2444 \pm 0.0015$ when using the method based on a set of 5 helium recombination lines to determine all of the H II region parameters. By more conventional methods, the same data gives $Y_p = 0.239 \pm 0.002$. As one can see, the ^4He data is clearly dominated by systematic uncertainties.

³We note that this method has been criticized as it relies on some ^4He data which is particularly uncertain, and these uncertainties have not been carried over into the error budget in the ^4He abundance [6].

There has been considerably less variability in the ${}^7\text{Li}$ data over the last several years. The ${}^7\text{Li}$ abundance is determined by the observation of Li in the atmospheres of old halo dwarf stars as a function of metallicity (in practice, the Fe abundance). The abundance used in [2] from the work in [7] continues to lead to the best estimate of the ${}^7\text{Li}$ abundance in the so called Spite plateau

$$y_7 \equiv \frac{{}^7\text{Li}}{\text{H}} = (1.6 \pm 0.07) \times 10^{-10} \quad (3)$$

where the error is statistical, again due to the large number of stars observed. If we employ the basic chemical evolution conclusion that metals increase linearly with time, we may infer this value to be indicative of the primordial Li abundance.

In [2], we noted that there are considerable systematic uncertainties in the plateau abundance. It is often questioned as to whether the Pop II stars have preserved their initial abundance of Li. While the detection of the more fragile isotope ${}^6\text{Li}$ in two of these stars may argue against a strong depletion of ${}^7\text{Li}$ [22, 9], it is difficult to exclude depletion of the order of a factor of two. Therefore it seems appropriate to allow for a wider range in ${}^7\text{Li}$ abundances in our likelihood analysis than was done in [2].

There has been some, albeit small, change in the D/H data from quasar absorption systems. Although the re-observation of the high D/H in [23] has been withdrawn, the original measurements [14] of this object still stand at the high value. More recently, a different system at the relatively low redshift of $z = 0.7$ was observed to yield a similar high value [16]

$$y_2 \equiv \text{D}/\text{H} = (2 \pm 0.5) \times 10^{-4}. \quad (4)$$

The low values of D/H in other such systems reported in [15] have since been refined to show slightly higher D/H values [17]

$$y_2 \equiv \text{D}/\text{H} = (3.4 \pm 0.3) \times 10^{-5}. \quad (5)$$

Though this value is still significantly lower than the high D/H value quoted above, the low value is now high enough that it contains sufficient overlap with the ranges of the other light elements considered to warrant its inclusion in our analysis.

3 Likelihood Functions

Monte Carlo and likelihood analyses have been discussed at great length in the context of BBN [24, 25, 26, 27, 28, 29, 3, 4, 2]. Since our likelihood analysis follows that of [4] and [2], we will be very brief here. The likelihood function for ${}^4\text{He}$, $L_4(N_\nu, \eta)$ is determined from a convolution of a theory function

$$L_{4,\text{Theory}}(Y, N_\nu, \eta) = \frac{1}{\sqrt{2\pi}\sigma_Y(N_\nu, \eta)} \exp\left(\frac{-(Y - Y_p(N_\nu, \eta))^2}{2\sigma_Y^2(N_\nu, \eta)}\right) \quad (6)$$

(where $Y_p(N_\nu, \eta)$ and $\sigma_Y(N_\nu, \eta)$ represent the results of the theoretical calculation) and an observational function

$$L_{4,\text{Obs}}(Y) = \frac{1}{\sqrt{2\pi}\sigma_{Y0}} \exp\left(\frac{-(Y - Y_0)^2}{2\sigma_{Y0}^2}\right) \quad (7)$$

where Y_0 and σ_{Y_0} characterize the observed distribution and are taken from Eqs. (2) and (3). The full likelihood function for ${}^4\text{He}$ is then given by

$$L_4(N_\nu, \eta) = \int dY L_{4,\text{Theory}}(Y, N_\nu, \eta) L_{4,\text{Obs}}(Y) \quad (8)$$

which can be integrated (assuming Gaussian errors as we have done) to give

$$L_4(N_\nu, \eta) = \frac{1}{\sqrt{2\pi(\sigma_Y^2(N_\nu, \eta) + \sigma_{Y_0}^2)}} \exp\left(\frac{-(Y_p(N_\nu, \eta) - Y_0)^2}{2(\sigma_Y^2(N_\nu, \eta) + \sigma_{Y_0}^2)}\right) \quad (9)$$

The likelihood functions for ${}^7\text{Li}$ and D are constructed in a similar manner. The quantities of interest in constraining the N_ν - η plane are the combined likelihood functions

$$L_{47} = L_4 \times L_7 \quad (10)$$

and

$$L_{247} = L_2 \times L_{47}. \quad (11)$$

Contours of constant L_{47} (or L_{247} when we include D in the analysis) represent equally likely points in the N_ν - η plane. Calculating the contour containing 95% of the volume under the L_{47} surface gives us the 95% likelihood region. From these contours we can then read off ranges of N_ν and η .

4 Results

Using the abundances in eqs (2,3) and adding the systematic errors to the statistical errors in quadrature we have a maximum likelihood distribution, L_{47} , which is shown in Figure 1a. This is very similar to our previous result based on the slightly lower value of Y_p . As one can see, L_{47} is double peaked. This is due to the minimum in the predicted lithium abundance as a function of η , as was discussed earlier. We also show in Figures 1b and 1c, the resulting likelihood distributions, L_{247} , when the high and low D/H values from Eqs. (4) and (5) are included.

The peaks of the distribution as well as the allowed ranges of η and N_ν are more easily discerned in the contour plots of Figure 2 which shows the 50%, 68% and 95% confidence level contours in L_{47} and L_{247} . The crosses show the location of the peaks of the likelihood functions. Note that L_{47} peaks at $N_\nu = 3.2$, (up slightly from the case with $Y_p = .234$) and $\eta_{10} = 1.85$. The second peak of L_{47} occurs at $N_\nu = 2.6$, $\eta_{10} = 3.6$. The 95% confidence level allows the following ranges in η and N_ν

$$\begin{aligned} 1.7 &\leq N_\nu \leq 4.3 \\ 1.4 &\leq \eta_{10} \leq 4.9 \end{aligned} \quad (12)$$

These results differ only slightly from those in [2].

Since L_2 picks out a small range of values of η , largely independent of N_ν , its effect on L_{247} is to eliminate one of the two peaks in L_{47} . With the high D/H value, L_{247} peaks at the slightly higher value $N_\nu = 3.3$, $\eta_{10} = 1.85$. In this case the 95% contour gives the ranges

$$\begin{aligned} 2.2 &\leq N_\nu \leq 4.4 \\ 1.4 &\leq \eta_{10} \leq 2.4 \end{aligned} \tag{13}$$

(Strictly speaking, η_{10} can also be in the range 3.2–3.5, with $2.5 \lesssim N_\nu \lesssim 2.9$ as can be seen by the 95% contour in Figure 2a. However this “peak” is almost completely invisible in Figure 1b.) The 95% CL ranges in N_ν for both L_{47} and L_{247} include values below the canonical value $N_\nu = 3$. Since one could argue that $N_\nu \geq 3$, we could use this condition as a Bayesian prior. This was done in [30] and in the present context in [2]. In the latter, the effect on the limit to N_ν was minor, and we do not repeat this analysis here.

In the case of low D/H, L_2 picks out a smaller value of $N_\nu = 2.4$ and a larger value of $\eta = 4.55$. The 95% CL upper limit is now $N_\nu < 3.2$, and the range for η is $3.9 < \eta_{10} < 5.4$. It is important to stress that with the increase in the determined value of D/H [17] in the low D/H systems, these abundances are now consistent with the standard model value of $N_\nu = 3$ at the 2σ level.

Although we feel that the above set of values represents the *current* best choices for the observational parameters, our real goal in this paper is to generalize these results for a wide range of possible primordial abundances. To begin with, we will fix $(\text{Li}/\text{H})_p$ from Eq. (3), and allow Y_p to vary from 0.225 – 0.250. In Figure 3, the positions of the two peaks of the likelihood function, L_{47} , are shown as functions of Y_p . The low- η peak is shown by the dashed curve, while the high- η peak is shown as dotted. The preferred value of $N_\nu = 3$, corresponds to a peak of the likelihood function either at $Y_p = 0.234$ at low $\eta_{10} = 1.8$ or at $Y_p = 0.243$ at $\eta_{10} = 3.6$ (very close to the value of Y_p quoted in [19]). Since the peaks of the likelihood function are of comparable height, no useful statistical information can be extracted concerning the relative likelihood of the two peaks. The 95% CL upper limit to N_ν as a function of Y_p is shown by the solid curve, and over the range in Y_p considered varies from 3.3 – 5.3. The fact that the peak value of N_ν (and its upper limit) increases with Y_p is easy to understand. The BBN production of ${}^4\text{He}$ increases with increasing N_ν . Thus for fixed Li/H, or fixed η , raising Y_p must be compensated for by raising N_ν in order to avoid moving the peak likelihood to higher values of η and therefore off of the ${}^7\text{Li}$ peak.

In Figure 4, we show the corresponding results with $(\text{Li}/\text{H})_p = 4.1 \times 10^{-10}$. In this case, we must assume that lithium was depleted by a factor of ~ 2.5 or 0.4 dex, corresponding to the upper limit derived in [9]. The effect of assuming a higher value for the primordial abundance of Li/H is that the two peaks in the likelihood function are split apart. Now the value of $N_\nu = 3$ occurs at $Y_p = 0.227$ at $\eta_{10} = 1.1$ (a very low value) and at $Y_p = 0.248$ and $\eta_{10} = 5.7$. The 95% CL upper limit on N_ν in this case can even extend up to 6 at $Y_p = 0.250$. In Figure 5, we show a compilation of the 95% CL upper limits to N_ν for different values of $(\text{Li}/\text{H})_p = 1.6, 2.0, 2.6, 3.2$, and 4.1×10^{-10} . The upper limit to N_ν can be approximated by a fit to our results which can be expressed as

$$N_\nu \lesssim 80Y_p + 2.5 \times 10^9 (\text{Li}/\text{H})_p - 15.15 \tag{14}$$

Finally we turn to the cases when D/H from quasar absorption systems are also considered in the analysis. For the high D/H given in Eq. (4), though there is formally still a high- η peak, the value of the likelihood function L_{247} there is so low that it barely falls within the 95% CL equal likelihood contour (see Figures 1b and 2a). Therefore we will ignore it here. In Figure 6, we show the peak value of N_ν and its upper limit for the two cases of $(\text{Li}/\text{H})_p = 1.6$ and 4.1×10^{-10} . These results differ only slightly from those shown in Figures 3 and 4. We note however, that overall the two values of Li/H do not give an equally good fit. For fixed D/H, the high value prefers a value of $\eta_{10} \simeq 1.8$ coinciding with the position of the low- η peak for $(\text{Li}/\text{H})_p = 1.6 \times 10^{-10}$. At higher Li/H, the low- η peak shifts to lower η diminishing the overlap with D/H. In fact at $(\text{Li}/\text{H})_p \gtrsim 3.8 \times 10^{-10}$, the likelihood function L_{247} takes peak values which would lie outside the 95% CL contour of the case $(\text{Li}/\text{H})_p = 1.6 \times 10^{-10}$. The relative values of the likelihood function L_{247} , on the low- η peak, for the five values of Li/H considered are shown in Figure 7. Contrary to our inability to statistically distinguish between the two peaks of L_{47} , the large variability in the values of L_{247} shown in Figure 7 are statistically relevant. Thus, as claimed in [4], if the high D/H could be confirmed, one could set a strong limit on the amount of ${}^7\text{Li}$ depletion in halo dwarf stars.

Since the low D/H value has come up somewhat, and since here we are considering the possibility for higher values of Y_p and $(\text{Li}/\text{H})_p$, the statistical treatment of the low D/H case is warranted. In Figure 8, we show the peak value and 95% CL upper limit from L_{247} when the low value of D/H is used from Eq. (5) with $(\text{Li}/\text{H})_p = 1.6 \times 10^{-10}$. The results are not significantly different in this case for the other choices of $(\text{Li}/\text{H})_p$. In order to obtain $N_\nu = 3$, one needs to go to ${}^4\text{He}$ abundances as high as $Y_p = 0.247$ with respect to the peak of the likelihood function. However, for $Y_p > 0.234$, the revised low value of D/H is compatible with ${}^4\text{He}$ and ${}^7\text{Li}$ at the 95% CL. The likelihood functions L_{247} are shown in Figure 9 for completeness.

5 Conclusions

We have generalized the full two-dimensional (in η and N_ν) likelihood analysis based on big bang nucleosynthesis for a wide range of possible primordial abundances of ${}^4\text{He}$ and ${}^7\text{Li}$. Allowing for full freedom in both the baryon-to-photon ratio, η , and the number of light particle degrees of freedom as characterized by the number of light, stable neutrinos, N_ν , we have updated the allowed range in η and N_ν based the higher value of $Y_p = 0.238 \pm 0.002 \pm 0.005$ from [20] which includes the recent data in [19]. The likelihood analysis based on ${}^4\text{He}$ and ${}^7\text{Li}$ yields the 95% CL upper limits: $N_\nu \leq 4.3$ and $\eta_{10} \leq 4.9$. The result for N_ν is only slightly altered, $N_\nu \leq 4.4$, when the high values of D/H observed in certain quasar absorption systems [14, 16] are included in the analysis. In this case, the upper limit to η_{10} is lowered to 2.4. Since the low values of D/H have been revised upward somewhat [15], they are now consistent with ${}^4\text{He}$ and ${}^7\text{Li}$ and $N_\nu = 3$ at the 95% CL. We have also shown how our results for the upper limit to N_ν depend on the specific choice for the primordial abundance of ${}^4\text{He}$ and ${}^7\text{Li}$. If we assume that the observational determination of ${}^7\text{Li}$ in halo stars is a true indicator the primordial abundance of ${}^7\text{Li}$, then the upper limit to N_ν varies from 3.3 – 5.3 for Y_p in the range 0.225 – 0.250. If on the other hand, ${}^7\text{Li}$ is depleted in

halo stars by as much as a factor of 2.5, then the upper limit to N_ν could extend up to 6 at $Y_p = 0.250$.

Acknowledgments We note that this work was begun in collaboration with David Schramm. This work was supported in part by DOE grant DE-FG02-94ER40823 at Minnesota.

References

- [1] G. Steigman, D.N. Schramm, and J. Gunn, Phys. Lett. **B66** (1977) 202.
- [2] K.A. Olive and D. Thomas, AstroPart. Phys. **7** (1997) 27.
- [3] B.D. Fields, and K.A. Olive, Phys. Lett. **B368** (1996) 103.
- [4] B.D. Fields, K. Kainulainen, K.A. Olive, and D. Thomas, New Astr. **1** (1996) 77.
- [5] C.J. Copi, D.N. Schramm, and M.S. Turner, Phys. Rev. **D55** (1997) 3389; N. Hata, G. Steigman, S. Bludman and P. Langacker, Phys. Rev. **D55** (1997) 540.
- [6] K.A. Olive, E. Skillman, and G. Steigman, Ap.J. **483** (1997) 788.
- [7] P. Molaro, F. Primas, and P. Bonifacio, A.A. **295** (1995) L47; P. Bonifacio and P. Molaro, MNRAS, **285** (1997) 847.
- [8] Y.I. Izotov, T.X. Thuan, and V.A. Lipovetsky, Ap.J. **435** (1994) 647; Ap.J.S. **108** (1997) 1.
- [9] M.H. Pinsonneault, T.P. Walker, G. Steigman, and V.K. Narayanan, Ap.J. (1998) submitted, astro-ph/9803073.
- [10] K.A. Olive, R.T. Rood, D.N. Schramm, J.W. Truran, and E. Vangioni-Flam, Ap.J. **444** (1995) 680; D. Galli, F. Palla, F. Ferrini, and U. Penco, Ap.J. **443** (1995) 536; D. Dearborn, G. Steigman, and M. Tosi, Ap.J. **465** (1996) 887; S.T. Scully, M. Cassé, K.A. Olive, D.N. Schramm, J. Truran, and E. Vangioni-Flam, Ap.J. **462** (1996) 960; K.A. Olive, S.T. Scully, D.N. Schramm, and J. Truran, Ap.J. **479** (1996) 752.
- [11] S. Scully, M. Cassé, K.A. Olive, E. Vangioni-Flam, Ap. J. **476** (1997) 521.
- [12] S.J. Lilly, O. Le Fevre, F. Hammer, and D. Crampton, Ap.J. **460** (1996) L1; P. Madau, H.C. Ferguson, M.E. Dickenson, M. Giavalisco, C.C. Steidel, and A. Fruchter, MNRAS **283** (1996) 1388; A.J. Connolly, A.S. Szalay, M. Dickenson, M.U. SubbaRao, and R.J. Brunner, Ap.J. **486** (1997) L11; M.J. Sawicki, H. Lin, and H.K.C. Yee, A.J. **113** (1997) 1.
- [13] M. Cassé, K.A. Olive, E. Vangioni-Flam, and J. Audouze, New Astronomy **3** (1998) 259.

- [14] R.F. Carswell, M. Rauch, R.J. Weymann, A.J. Cooke, and J.K. Webb, MNRAS **268** (1994) L1; A. Songaila, L.L. Cowie, C. Hogan, and M. Rugers, Nature **368** (1994) 599.
- [15] D. Tytler, X.-M. Fan, and S. Burles, Nature **381** (1996) 207; S. Burles and D. Tytler, Ap.J. **460** (1996) 584.
- [16] J.K. Webb, R.F. Carswell, K.M. Lanzetta, R. Ferlet, M. Lemoine, A. Vidal-Madjar, and D.V. Bowen, Nature **388** (1997) 250; D. Tytler et al., astro-ph/9810217 (1998).
- [17] S. Burles and D. Tytler, Ap.J. **499** (1998) 699; Ap.J. **507** (1998) 732.
- [18] C. Copi, K.A. Olive, and D.N. Schramm, Proc. Nat. Ac. Sci. **95** (1998) 2758, astro-ph/9606156.
- [19] Y.I. Izotov, and T.X. Thuan, ApJ, **500** (1998) 188.
- [20] B.D. Fields and K.A. Olive, Ap.J. **506** (1998) 177.
- [21] B.E.J. Pagel, E.A. Simonson, R.J. Terlevich and M. Edmunds, MNRAS **255** (1992) 325; E. Skillman, and R.C. Kennicutt, ApJ, 411 (1993) 655; E. Skillman, R.J. Terlevich, R.C. Kennicutt, D.R. Garnett, and E. Terlevich, ApJ, 431(1994) 172.
- [22] G. Steigman, B. Fields, K.A. Olive, D.N. Schramm, and T.P. Walker, Ap.J. **415** (1993) L35; M. Lemoine, D.N. Schramm, J.W. Truran, and C.J. Copi, Ap.J. **478** (1997) 554; B.D. Fields and K.A. Olive, astro-ph/9811183, New Astronomy, in press (1998).
- [23] M. Rugers and C.J. Hogan, Ap.J. **459** (1996) L1.
- [24] L.M. Krauss and P. Romanelli, ApJ, **358** (1990) 47.
- [25] M. Smith, L. Kawano, and R.A. Malaney, Ap.J. Supp., **85** (1993) 219.
- [26] P.J. Kernan and L.M. Krauss, Phys. Rev. Lett. **72** (1994) 3309.
- [27] L.M. Krauss and P.J. Kernan, Phys. Lett. **B347** (1995) 347.
- [28] N. Hata, R.J. Scherrer, G. Steigman, D. Thomas, and T.P. Walker, Ap.J., **458** (1996) 637.
- [29] N. Hata, R. J. Scherrer, G. Steigman, D. Thomas, T. P. Walker, S. Bludman and P. Langacker, Phys. Rev. Lett. **75** (1995) 3977.
- [30] K.A. Olive and G. Steigman, Phys. Lett. **B354** (1995) 357.

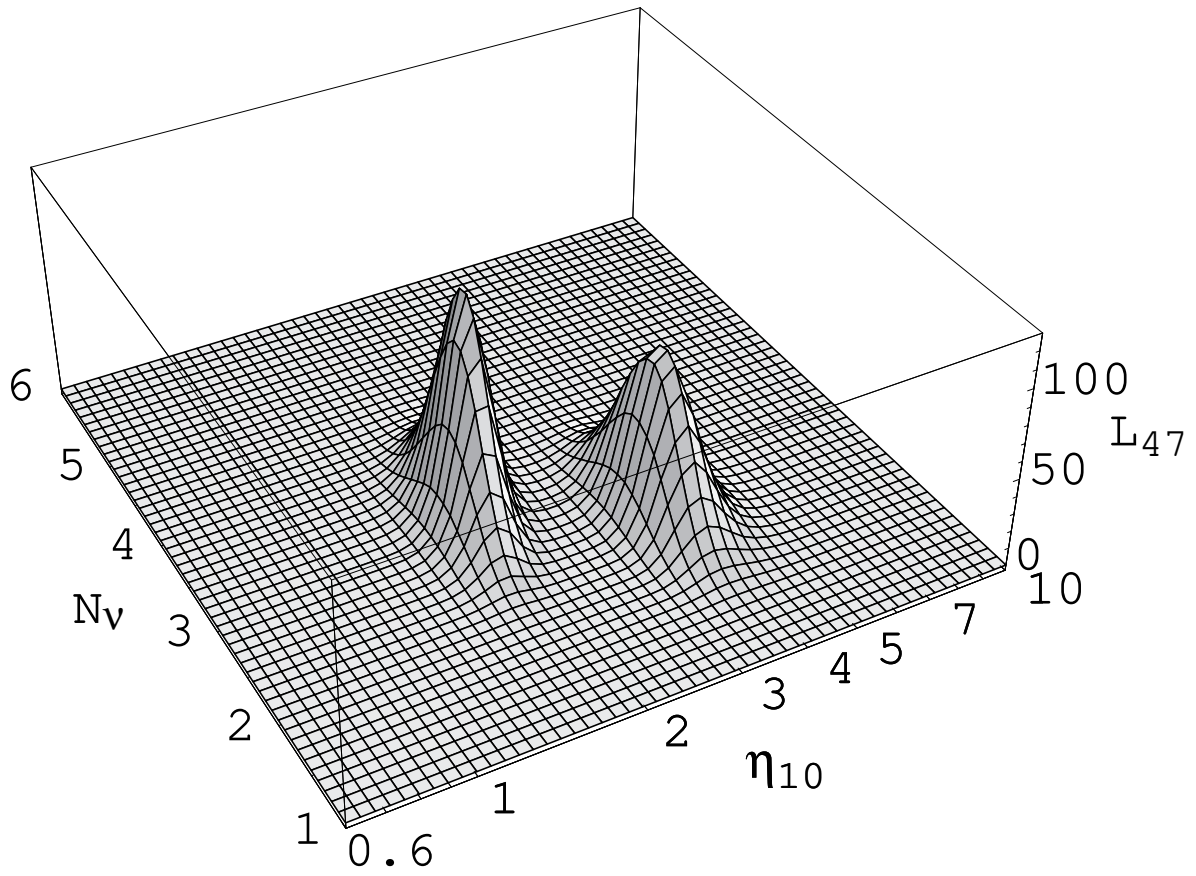


Figure 1: (a) $L_{47}(N_{\nu}, \eta)$ for observed abundances given by eqs. (2 and 3).

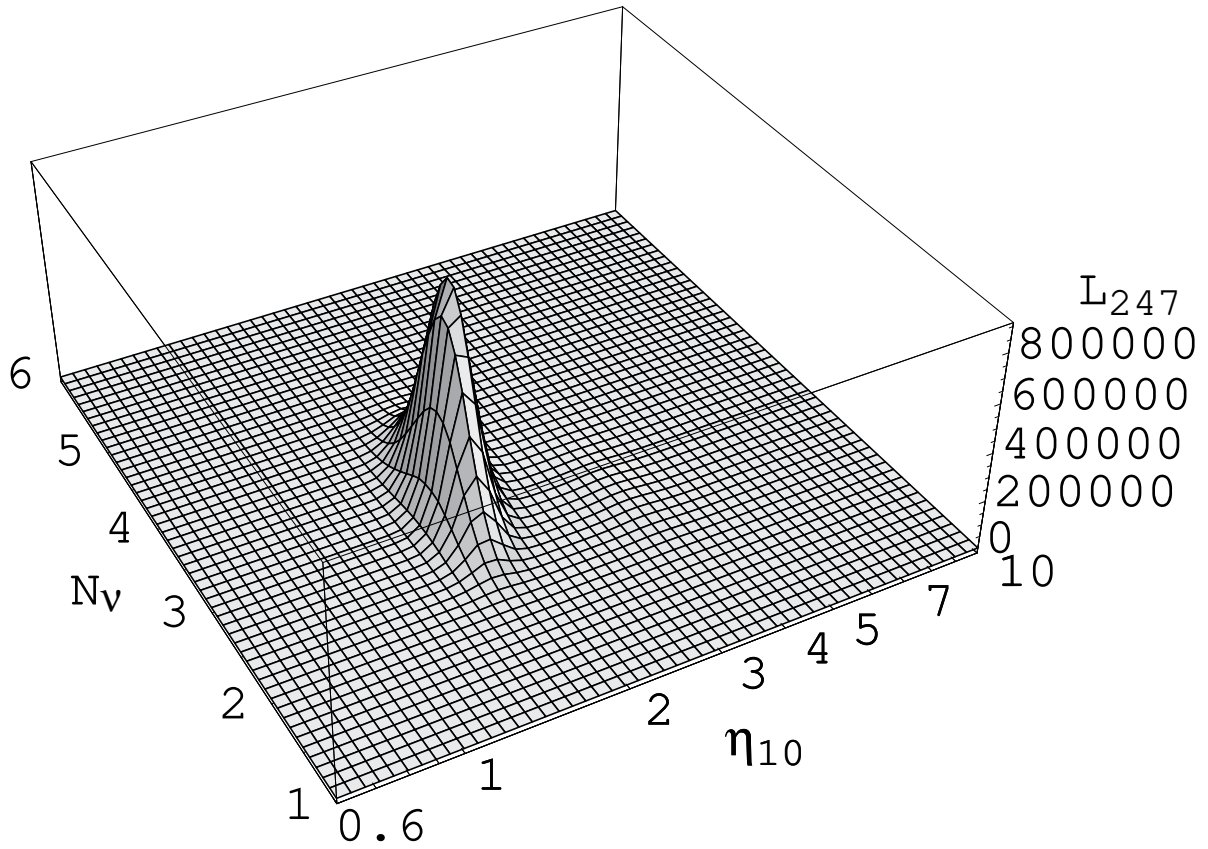


Figure 1: (b) $L_{247}(N_{\nu}, \eta)$ for observed abundances given by eqs. (2, 3, and 4).

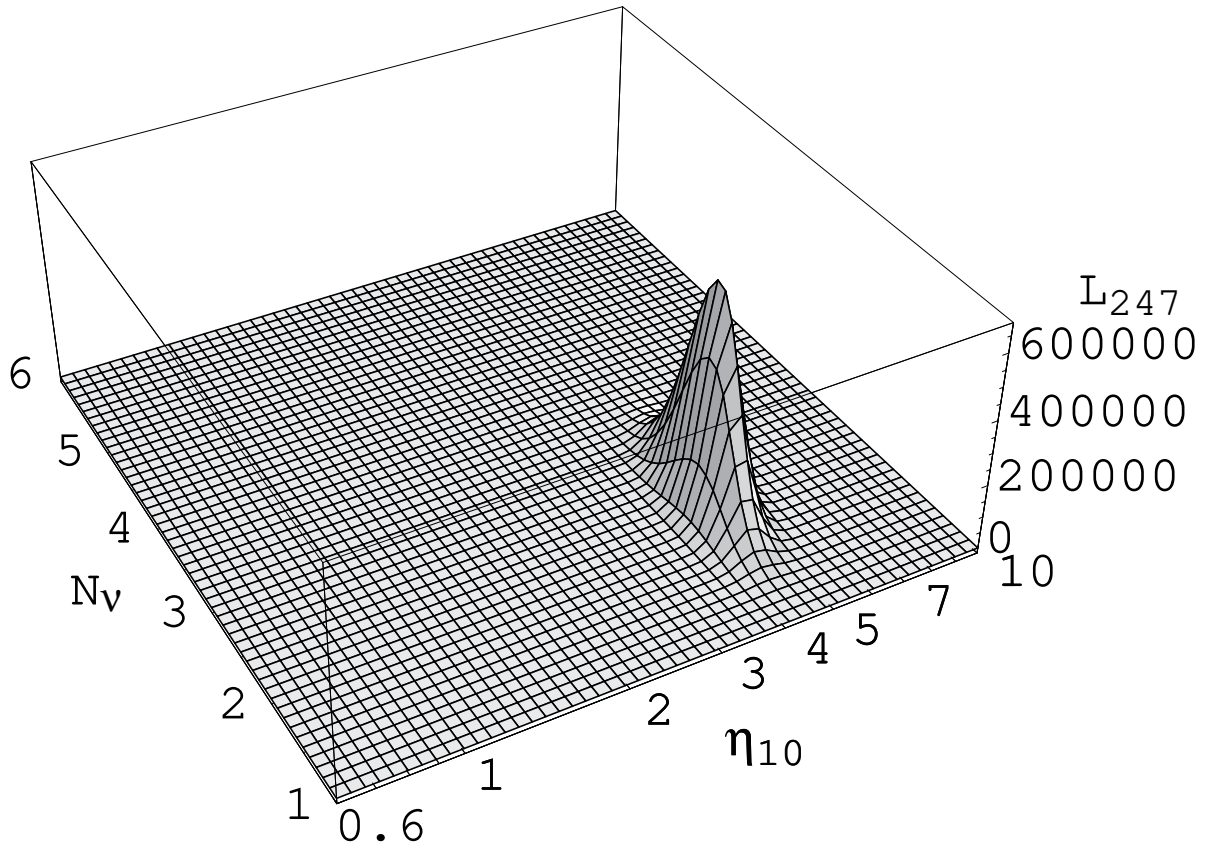


Figure 1: (c) $L_{247}(N_{\nu}, \eta)$ for observed abundances given by eqs. (2, 3, and 5).

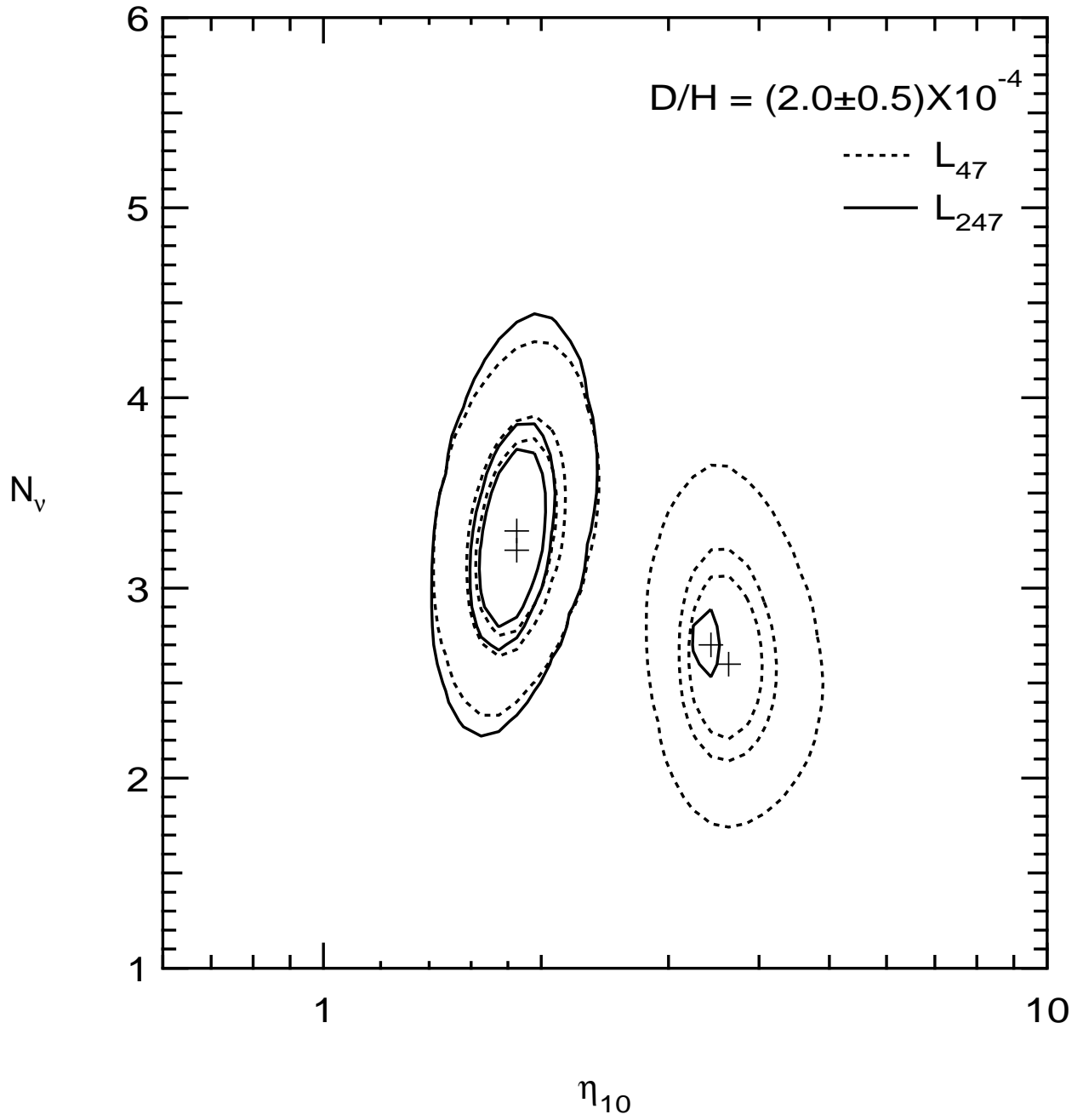


Figure 2: (a) 50%, 68% & 95% C.L. contours of L_{47} and L_{247} where observed abundances are given by eqs. (2, 3, and 4).

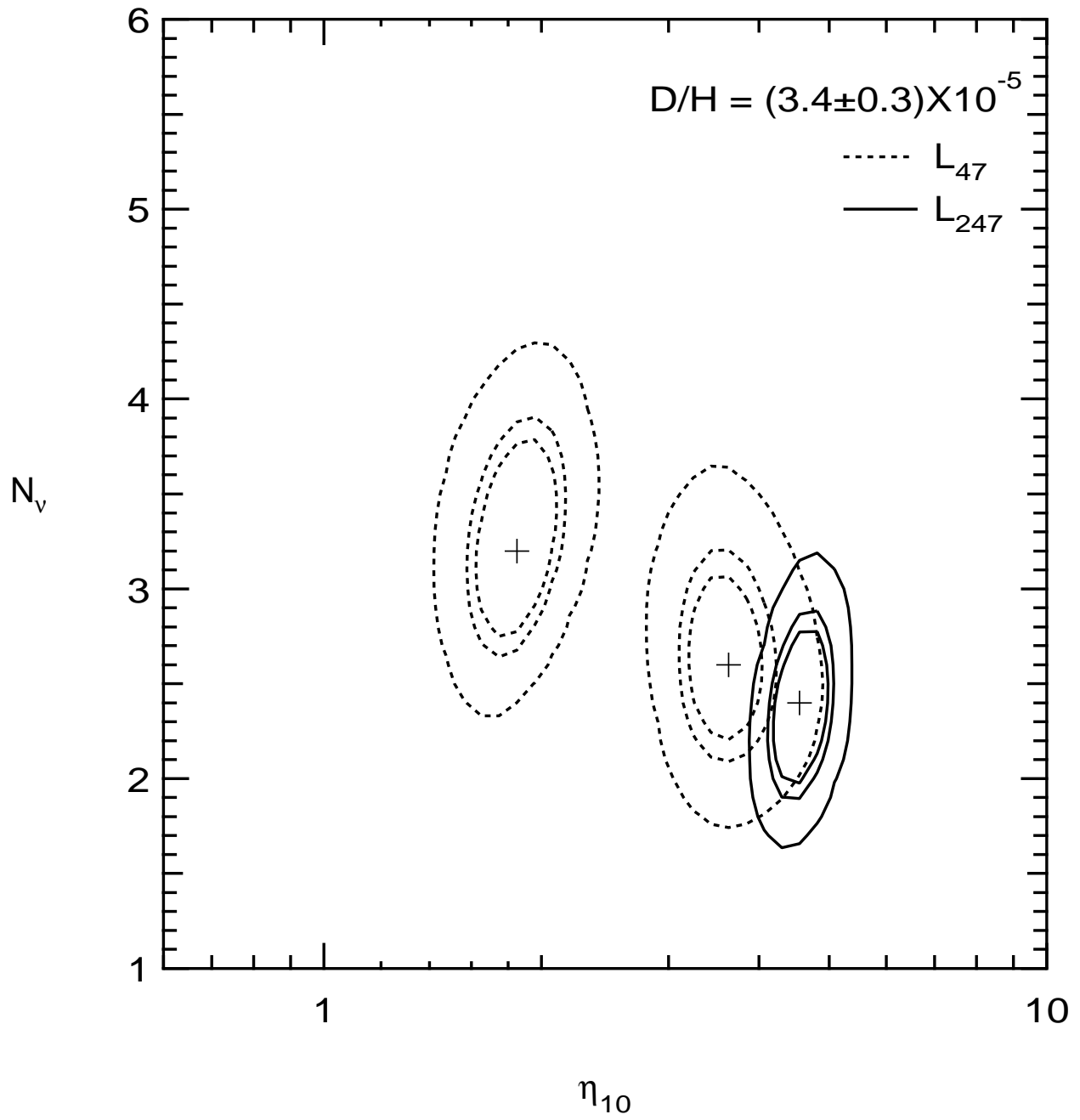


Figure 2: (b) 50%, 68% & 95% C.L. contours of L_{47} and L_{247} where observed abundances are given by eqs. (2, 3, and 5).

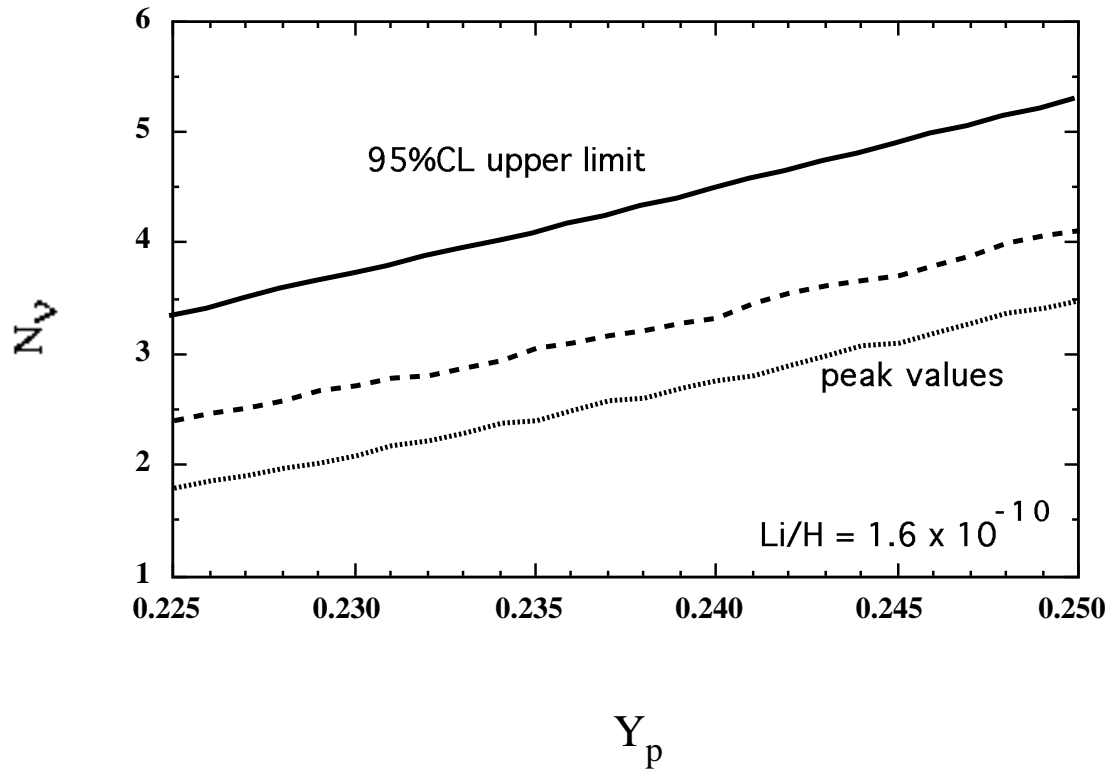


Figure 3: The position of the value of N_ν along the low- η peak (dashed) and high- η peak (dotted) of the likelihood function L_{47} as function of Y_p . The solid curve shows the 95% CL upper limit to N_ν as a function of Y_p . The value of $(\text{Li}/\text{H})_p = 1.6 \times 10^{-10}$ has been fixed.

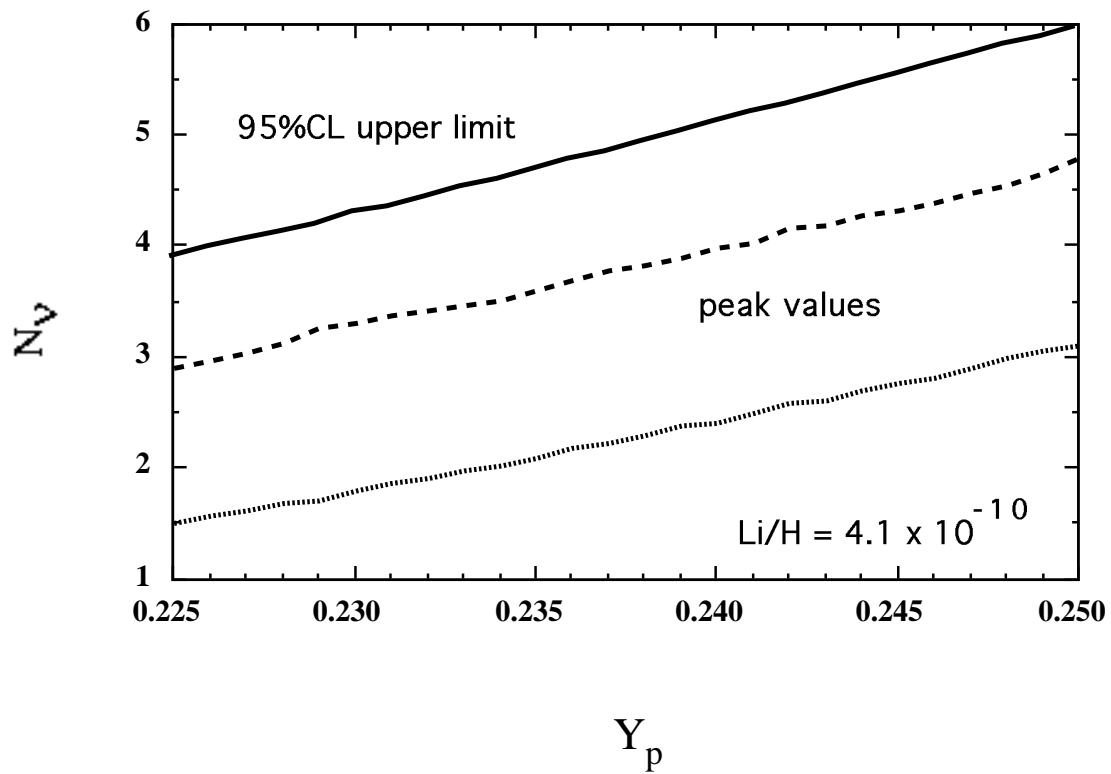


Figure 4: As in Figure 3 with $(\text{Li}/\text{H})_p = 4.1 \times 10^{-10}$.

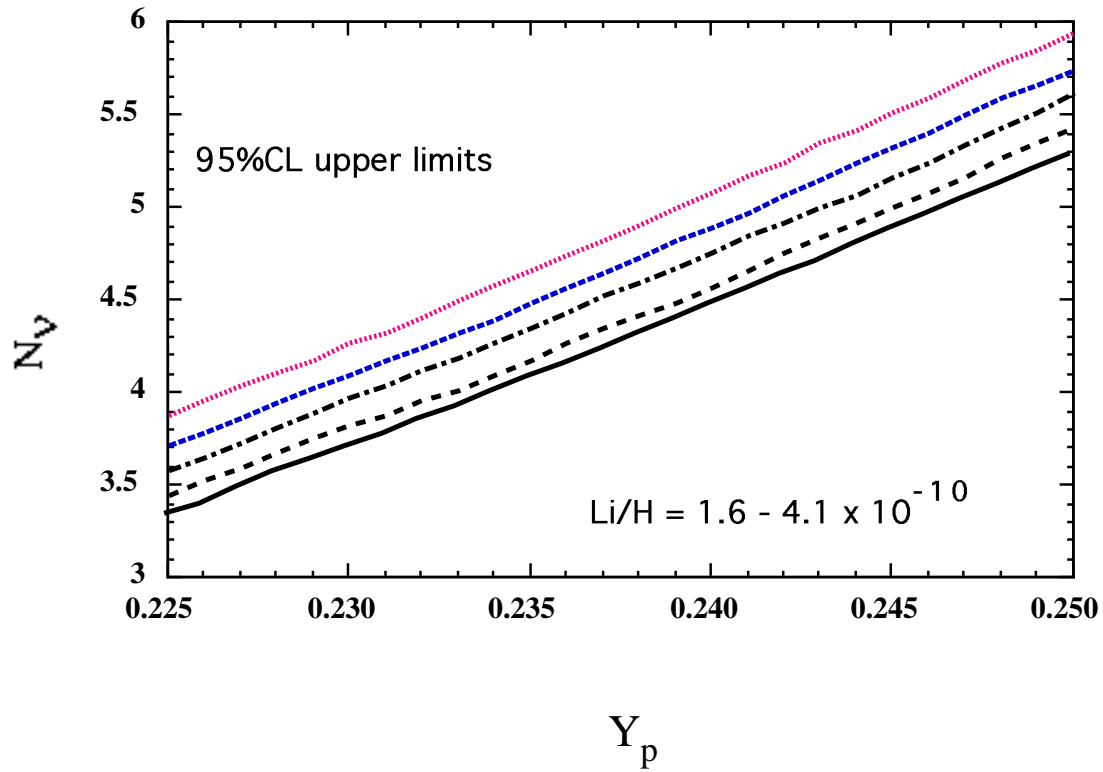


Figure 5: Summary of the upper limits to N_ν for $(\text{Li}/\text{H})_p = 1.6, 2.0, 2.6, 3.2,$ and 4.1×10^{-10} as a function of Y_p . The lowest curve corresponds to $(\text{Li}/\text{H})_p = 1.6 \times 10^{-10}$ and the limits on N_ν increase with $(\text{Li}/\text{H})_p$.

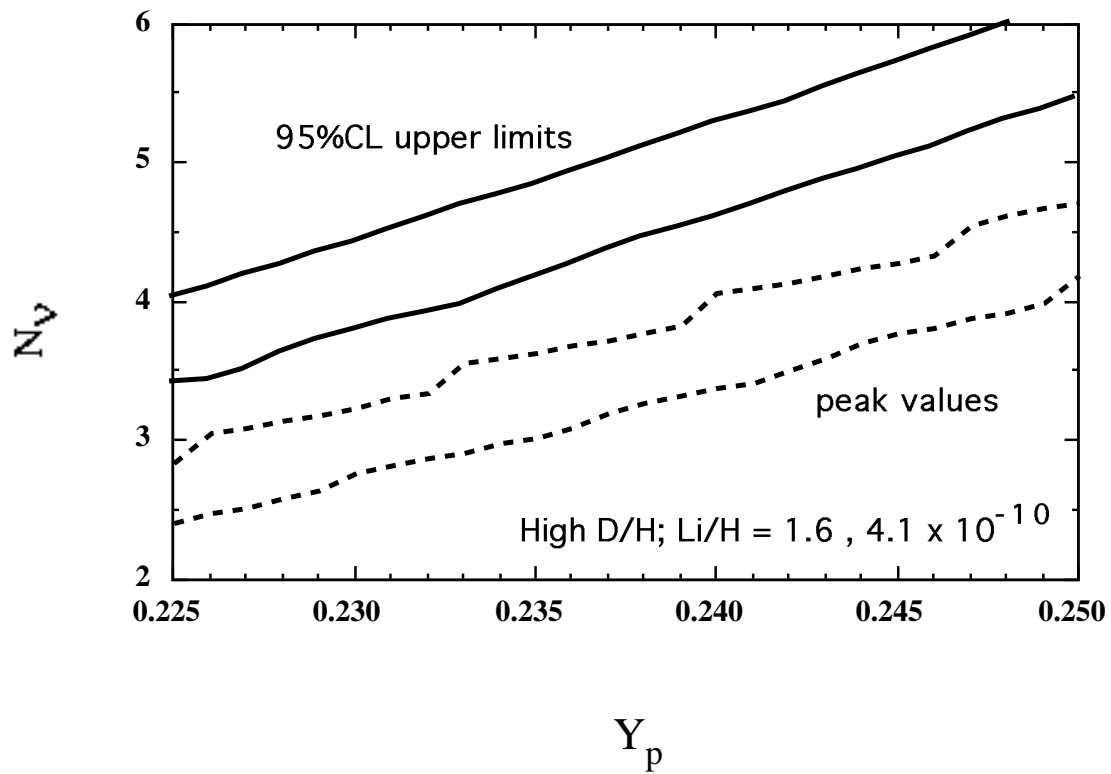


Figure 6: As in Figures 3 and 4 based on the likelihood function L_{247} which includes high D/H from quasar absorption systems.

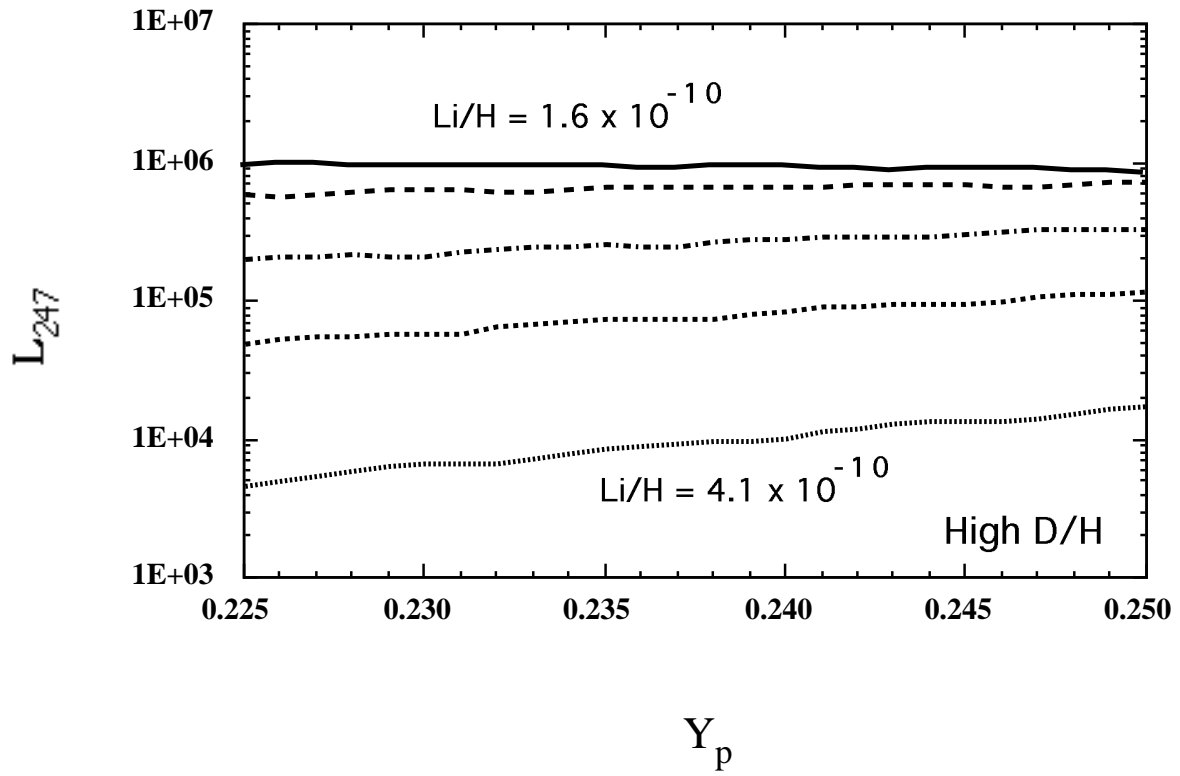


Figure 7: Relative values of the likelihood function L_{247} , on the low- η peak, for the five choices of $(\text{Li}/\text{H})_p$ in Figure 5.

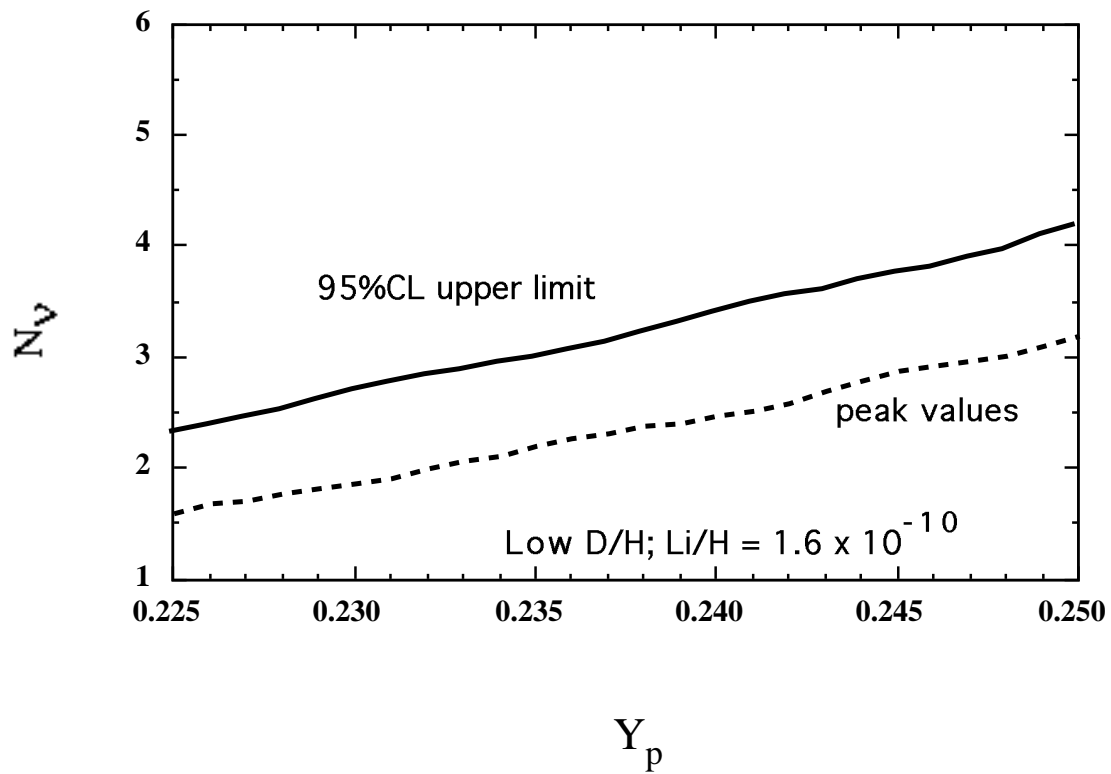


Figure 8: As in Figure 6 for low D/H from quasar absorption systems.

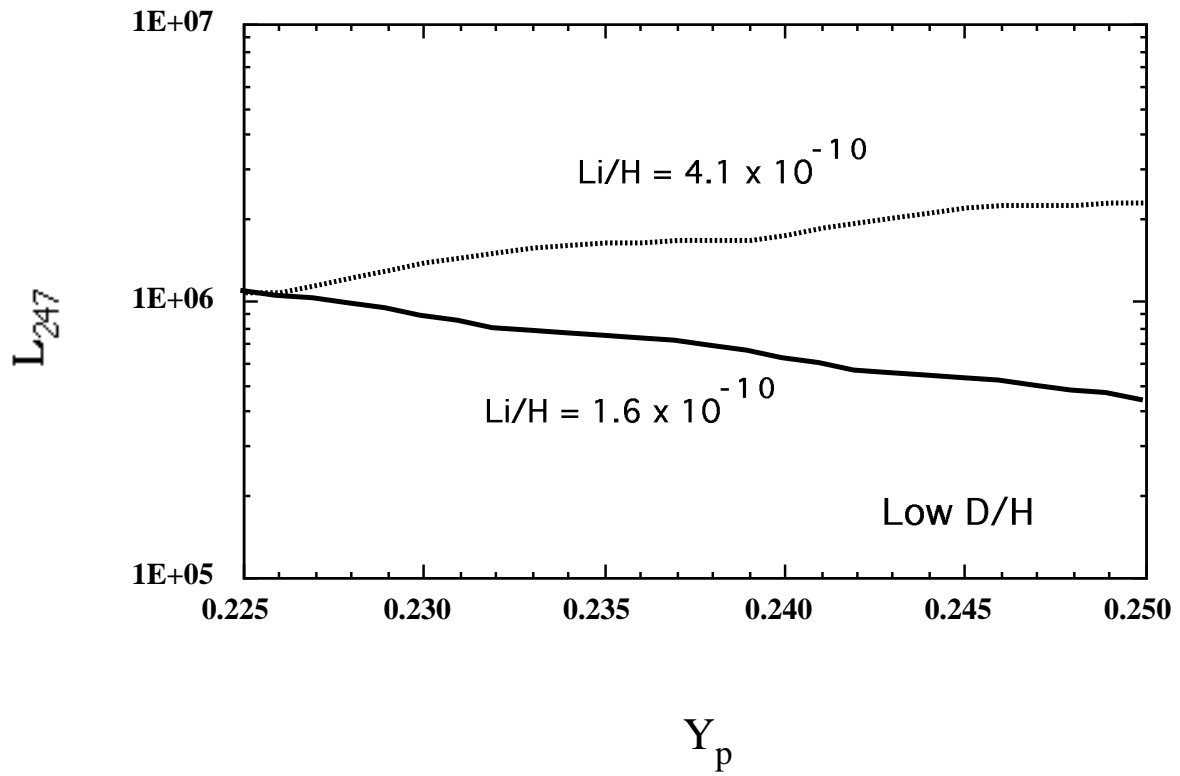


Figure 9: As in Figure 7 for low D/H from quasar absorption systems.